ELECTROMAGNETIC HEATING ASSISTED ENERGY STORAGE: LABORATORY STUDY

Jash Kalpoe

Delft University of Technology

ELECTROMAGNETIC HEATING ASSISTED ENERGY STORAGE: LABORATORY STUDY

By

JASH G. C. KALPOE

in partial fulfilment of the requirements for the degree of

Master of Science

in Applied Earth Sciences

at the Delft University of Technology

to be defended publicly on Thursday November 25, 2021

Student number:	4012038	
Supervisors:	Prof. Dr. P.L.J. Zitha	TU Delft
	Ing. H.K.J. Heller	TU Delft
Thesis Committee:	Dr. K.H.A.A. Wolf	TU Delft
	Dr. S. Jones	TU Delft
	Prof. G. Chapiro	Federal University of Juiz de Fora

ABSTRACT

Energy storage is increasingly becoming a possible solution worldwide to aid the energy supply and demand. The objective of this study is to determine whether thermal energy storage can be effectively and efficiently achieved by ways of electromagnetic (EM) radiation. To serve this purpose, an experimental setup was designed in order to subject core flooding experiments to EM heating using a MW source. Temperature data is obtained and used to construct temperature profiles as well as energy absorption and storage profiles. The experiments vary from EM radiation under no flow conditions to experiments inducing flow in order to determine the effect of flow on energy absorption and storage amounts. The results obtained illustrate that a significant amount of energy is absorbed by the core and that the introduction of flow at the chosen flowrates during EM heating does not diminish the energy absorption ability of water inside the core. Flow does however increase the rate of energy decline within the core when EM heating is stopped thus reducing the amount of energy stored. Nevertheless, around 40% of the energy absorbed after 150 seconds of EM heating is stored in the core after a cooling period of 60 minutes. This amount declines significantly when flow in implemented throughout heating and cooling. Even though the experimental setup performed accordingly, the large amounts of thermal energy losses are an area that should be subject to improvement. When this technology is implemented in reservoirs or aquifers, the MW antenna is placed in the pay zone. This results in lower energy losses due to the over- and underlying formations functioning as insulation. Subject to improvements, this study concludes that EM stimulated core flooding is a legitimate and viable technology with significant potential for thermal energy storage purposes.

ACKNOWLEDGEMENTS

I would first like to show my gratitude to my supervisor, Prof. Dr. Pacelli Zitha, for his support and motivation during this time. Your knowledge on the subject and in general, along with your insightful feedback, were fundamental to my thought process and overall approach to the numerous challenges.

I would like to acknowledge Ing. Karel Heller, Ing. Michiel Slob, Ing. Paul Vermeulen and the rest of the laboratory staff for their insights into the subject at hand and for help with the building and performance of the experimental setup in the lab. I have enjoyed the time I have spent in the lab and appreciate getting the opportunity and the learning experience.

I would like to express my sincere gratitude to my parents and my sister for their unconditional support during my studies and providing me with the motivation and support to achieve what I wanted to achieve.

And last but definitely not least I would like to thank my girlfriend for her support during this time, for being who she is and for pushing me to be my best self.

CONTENT

LIST OF SYMBOLS

Symbol	Remark	Unit
A	Area	m^2
c_α	Specific heat capacity of a substance	*J/kg K*
c_w	Specific heat capacity, water	*J/kg K*
c_s	Specific heat capacity, sandstone	*J/kg K*
D	Core diameter	*m*
E_α	Energy transferred to substance α	*J*
E_g	Energy generated by the MW	*J*
E_w	Energy absorbed by water through radiation	*J*
E_s	Energy transferred to the rock through conduction	*J*
E_d	Energy losses between cycles	*J*
E_{st}	Energy stored in the core	*J*
f	Microwave frequency	*Hz*
k	Absolute permeability	m^2
L	Length	*m*
m	Mass	*kg*
m_α	Mass of a substance	*kg*
m_w	Mass of water	*kg*
m_s	Mass of sandstone	*kg*
n	Number of EM cycles	-
P	Pressure	*Pa*
ΔP	Pressure difference	*Pa*
PV	Pore volume	m^3
Q	Fluid flowrate	m^3/s
q	Water injection rate	m^3/s
S_w	Water saturation	-

T	Measured temperature by thermocouple	K
Ti	Initial room temperature	K
ΔT	Temperature change or difference	K
t	Time	s
Δt_c	EM full cycle duration	s
Δt_g	Effective on-time of EM radiation, per cycle	s
Δt_o	EM off-cycle time, per cycle	s
Δt_d	EM delay, per cycle	s
μ	Viscosity	$Pa.s$
μ_w	Water viscosity	$Pa.s$
V	Volume	m^3
W	Microwave power	W
λ	Wavelength	m
ρ	Density	kg/m^3
ρ_w	Density of water	kg/m^3
ρ_s	Density of sandstone	kg/m^3
ϕ	Porosity	-

NOMENCLATURE

Abbreviations

EM	Electromagnetic
HDPE	High-density polyethylene
MW	Microwave
PEEK	Polyether-ether-ketone
PET	Polyethylene terephthalate

LIST OF FIGURES

LIST OF TABLES

1 INTRODUCTION

Methods for generating renewable energy have developed rapidly in the recent few decades in order to meet the growing energy demand and reduce greenhouse gas emissions inherent in the combustion of natural hydrocarbons. Technologies such as photo-voltaic solar panels and wind-turbines are becoming a more prominent part of the energy mix of many countries. However, these technologies face issues such as significant energy losses and discontinuous availability and supply that still need solving. Their dependence on solar and weather conditions for energy generation (supply) makes them uncontrollable and unpredictable at a given time whereas energy usage (demand) may vary in time (Dorsey et al., 2019, as cited in Almeida et al., 2021). Often, energy generated now is needed later.

Thermal energy storage systems and technologies can potentially provide a solution to this problem. The generated renewable energy is safely stored over time while significantly minimizing thermal energy losses during storage. Supply may be adjusted to the requirements and demands at any given time. One technology which provides this option is the usage of electromagnetic (EM) radiation. This method was first reported by Abernethy (1976). It is a frequency dependent radiation technology that uses electromagnetism, preferably at high frequencies, which causes the generation of heat when subjected to an energy absorbing medium.

The application of EM radiation for thermal enhanced oil recovery (EOR) was investigated by several authors in the past. The method consists of water flooding where water is heated in situ using a radiation antenna installed at the bottom of the well. This allows the energy to be injected directly into the pay zone, which minimizes energy losses to the surrounding rock and soil (Fanchi, 1990). Hot water imparts its thermal energy to the oil thus decreasing its viscosity and increasing its production. Several past experimental studies have revealed that EM-heating assisted water flooding of oil-bearing sandstones increases oil recovery by up to 37.0 (Paz et al., 2017).

The potential of energy storage by EM heating was investigated by numerical simulation of simultaneous water injection into an inverted five-spot model reservoir and EM heating (Almeida et al., 2021). The authors demonstrated that the energy could be stored with an efficiency of more than 70%. However, lab experiments providing data concerning the potential of energy storage by EM heating are scarce in literature. This study is an attempt to fill this gap. Multiple experiments are conducted on vials containing water as well as on a specially designed setup combining a core-flooding and domestic microwave generator operating at high frequency (2.45 GHz). The objective of this study is to characterize and investigate the EM heating of water contained in a vial and in a model natural sandstone and the resulting energy absorption and storage capacity of this technology. Furthermore, the impact of flow of water on this method is examined in detail.

2 METHODOLOGY

2.1 EM radiation background

The molecular configuration of water, illustrated in Fig. 1, is dipolar in nature which leads to water being a useful dielectric material. Due to the fact that EM radiation is made up of an oscillating electric and magnetic field (Tran and Zitha, 2009) and water being a useful dielectric material, a physical oscillating effect on the water molecule occurs when exposed to EM radiation. Based on the radiation frequency the vibration of the molecules leads to friction which in turn leads to the generation of heat. When radiating at high frequency, this dielectric heating effect is more intense and dominant (Samanta, 2007).

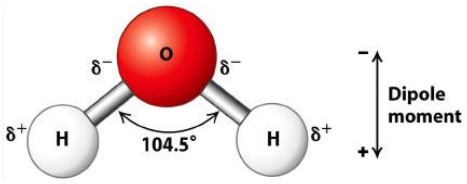

Figure 1: Water molecule configuration. *(Molecular Cell Biology, Sixth Edition, W. H. and Company 2008)*

2.2 Physical model

For the EM characterization experiments a vial containing water is situated in front of the MW antenna and heated by EM radiation. For the core experiments a cylindrical homogeneous and isotropic Bentheimer sandstone core with a cross-sectional area *A*, length *L*, porosity and permeability *k* is placed in front of the antenna of the EM heating system. Water at initial room temperature *Ti*, with viscosity μ and liquid-phase density ρ, is injected into the core at a flow rate *Q* until the core is fully saturated (S_w = 1). The core is then subjected to EM radiation under static (no flow) and dynamic (including flow) conditions.

2.3 Modeling of the EM heating process

2.3.1 Main assumptions

For the modelling of the EM heating process the following assumption were made:

1. The rock and fluid are incompressible and their densities are independent of temperature within the range investigated. They are therefore considered constants.

2. During injection, one-dimensional steady-state flow is assumed which means the pressure gradient inside the core is constant. Flow is according to Darcy's law.
3. During heat transfer thermal expansion of the fluid and rock is assumed to be negligible.
4. Energy generated by the EM source is absorbed by water in the porous medium by ways of radiation.
5. Energy transfer from water in the porous medium to the rock occurs by ways of conduction.
6. Furthermore, water and rock are in instant thermal equilibrium (at the same temperature) during EM heating and cooling-off due to the fact that heat transfer between water and rock is assumed to be instantaneous.
7. Due to the high permeability of this sandstone (2 Darcy), capillary effects in the pores are assumed to be insignificant during these experiments.

2.3.2 Model equations

Under steady-state flow conditions, taking into account the above assumptions, the EM heating process can be described by the following equations, expressing mass balance (1), energy balance (2), and Darcy's equation (3):

$$\rho_w V_{in} - \rho_w V_{out} = 0 \tag{1}$$

$$E_g - (E_d + E_w + E_s) = 0 \tag{2}$$

$$\mathrm{Q} = \frac{k}{\mu} A \frac{\Delta P}{L} \tag{3}$$

The energy absorbed by water and sandstone is determined by using the following thermodynamic equation for thermal energy content of a liquid or solid:

$$E_\alpha = m_\alpha \, c_\alpha \, \Delta T, \tag{4}$$

Here ΔT [℃] constitutes to the difference between Ti [℃] and T [℃], at the specific thermocouple positions.

2.3.3 Microwave power generation

The microwave generator used in this study supplies EM energy according to the cycle timing illustrated in Fig. 2.

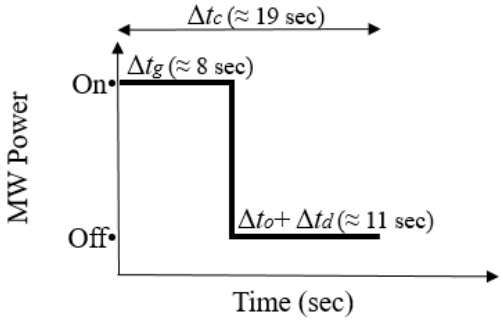

Figure 2: Timing subdivision for one MW cycle

The total energy generated by the MW source during a certain time of experimenting corresponds to the duration of consecutive cycles, each with duration Δt_c. Each cycle consists of an on period, where the EM is actually emitted, followed by an off period. A significant delay occurs between on- and off-cycles which has to be corrected for in order to obtain the actual time of radiation. Therefore, Δt_g for each MW-cycle, is determined by subtracting Δt_o and Δt_d from each full cycle time (5).

$$\Delta t_g = \Delta t_c - (\Delta t_o + \Delta t_d) \tag{5}$$

By obtaining the effective MW on-time per cycle as well as cumulatively for all cycles, it can be implemented to determine the amount of energy generated by the MW source, E_g. This is obtained by multiplying the MW power W by Δt_g. Implementing this for n-cycles the amount of energy generated during the full time of EM heating can be obtained (6).

$$E_g = \sum_{i=1}^{n} \int_{0}^{t_{gi}} W(t)\, dt \tag{6}$$

The energy generated by the MW source reaches the core and is partly absorbed by water. E_w, is determined by specifying (4) for water thus obtaining (7). Energy transfer from water to the solid is determined by (8).

$$E_w = m_w c_w \sum_{cycle\ 1}^{n} \Delta T \tag{7}$$

$$E_s = m_s c_s \sum_{cycle\ 1}^{n} \Delta T \tag{8}$$

During EM heating not all generated energy is absorbed by water. A significant amount is lost to the surroundings. By subtracting the sum of the energy absorbed by water and the rock from the energy generated by the MW, E_d can be calculated as follows:

$$E_d = E_g - (E_w + E_s) \tag{9}$$

Substituting (6), (7) and (8) into the energy balance equation (2), it can be rewritten as:

$$\sum_{i=1}^{n} \int_{0}^{t_{gi}} W(t)\, dt - (E_d + m_w c_w \sum_{cycle\ 1}^{n} \Delta T + m_s c_s \sum_{cycle\ 1}^{n} \Delta T) = 0 \tag{10}$$

After EM heating, a one hour cooling off period is started to determine the amount and rate of thermal energy decline in the system as a whole, E_{dc}, thus knowing the amount of energy stored, E_{st}. The energy stored in the core is obtained using (11).

$$E_{st} = (E_w + E_s) - E_{dc} \tag{11}$$

$$E_{dc} = (m_w c_w - \Delta T) + (m_s c_s - \Delta T) \tag{12}$$

3 EXPERIMENTS

3.1 Materials and methods

3.1.1 Injection fluid preparation

Tap water (ρ_w = 1000 [kg/m^3], μ_w = 0.001 [Pa.s] and c_w = 4182 [J/kg•K]) is used for all experiments related to this study. This is due to the fact that the main dissolved minerals in tap water are Calcium and Chloride at the amounts of 49 mg/L and 51 mg/L (Lenntech Water Treatment Solutions), respectively. The influence of these minerals at these concentrations is expected to be negligible when injected into the sandstone core. For the water flooding experiments the tap water is degassed beforehand in order to limit bubble formation in the pump and tubes when injecting into the core as well as to minimize bubble formation inside the core when inducing EM heating.

3.1.2 Porous medium

A Bentheimer sandstone core is used as the porous medium for experiments. Internal structural properties such as constant grain size distribution, porosity, permeability, few amounts of minerals as well as its lateral continuity and

homogeneous block-scale internal structure makes it a widely used sandstone for various lab experiments and studies (Peksa et al., 2015). The core has a length L of 17.0 ± 0.1 cm and diameter D of 4.0 ± 0.1 cm. The rock has a porosity ϕ of approximately 25 % and a permeability *k* of 1.91 ± 0.01 D. The pore volume PV is 40.5 ± 0.1 mL.

Table 1: Core parameters

Symbol	Parameter	Value	Unit
ϕ	Core porosity	0.25 ± 0.02	*[-]*
k	Core absolute permeability	1.91 ± 0.01	*[D]*
PV	Core pore volume	40.5 ± 0.1	*[mL]*
L	Length of the core	0.17 ± 0.001	*[m]*
d	Core diameter	0.04 ± 0.001	*[m]*
A	Cross sectional area of the core	0.00126	*[m^2]*
ρ_s	Bentheimer SST density	2650	*[kg/m^3]*
c_s	Bentheimer SST specific heat capacity	730	*[J/kg K]*

3.1.3 EM heating details

During the experiments the average time of one full cycle of EM heating corresponds to 19.0 +/- 1.0 seconds, the off-cycle time corresponds to 6.0 +/- 1.0 seconds and the delay-time corresponds to 5.0 +/- 1.0 seconds. Therefore the effective MW on-time of heating is determined to be 8.0 +/- 1.0 seconds. This can be seen in Fig. 2. Subsequently, for eight cycles cumulatively this becomes 64.0 ± 1.0 seconds of actual EM heating. During heating, thermal energy losses occur in between heating cycles. This is accounted for when determining temperature profiles. The cause of these losses can be multiple. It can be related to flawed insulation of the core holder, waveguide or faraday cage. Lower amounts of energy absorbed may imply that the performance of the MW is not optimal. In this study this distinction is not made, energy losses are assumed to be due to the insulation of the materials used with the MW working at optimal capacity. Immediately after 150 seconds of EM heating the MW is turned off starting a 60 minute cooling off period.

3.2 EM Characterization setup and procedure

Before performing core experiments, the radiation field in absence of porous media is characterized. This concerns the use of two degassed tap water filled plastic polyethylene vials with different dimensions and slight material

differences (Table 2). Vial 1 is made of PET material whereas vial 2 consists of HDPE material. The main differences between these two plastics are the rigidity, transparency and the temperature resistance intervals. These differences are deemed to be very small and therefore insignificant to the purpose they serve. The main and most important difference between the vials is the body of water each vial can contain. 125 mL for vial 1 compared to 175 mL for vial 2. The vials, filled with tap water, are placed in front of the waveguide at increasing distances and heated for 150 seconds. The distances used are 0 – 20 cm with 5 cm increments, as demonstrated in Fig. 3. These positions correspond to the assigned tags P1, P2, P3, P4 and P5 with P1 located at 0 cm distance to the wave guide and P5 located at 20 cm distance to the wave guide (Experiment 1). The temperature of the static (non-stirred) water is measured and used to determine the amount of energy absorbed. The measurement is done by using a handheld Ni-Cr/Ni-Al thermocouple, where the placement of the thermocouple in the vial, by hand, has to be kept consistent. The experiment is repeated at 0 cm (P1.S), 10 cm (P3.S) and 20 cm (P5.S) with stirring induced (Experiment 2). In this case the water in the vials is stirred after heating before measuring the temperature. Stirring is added to gain insight into the possible difference in temperature profiles and energy absorption between static and dynamic water heating. Table 2 provides the properties of the vials used and Table 3 gives the positions of the vials in front of the MW source during experiments 1 and 2.

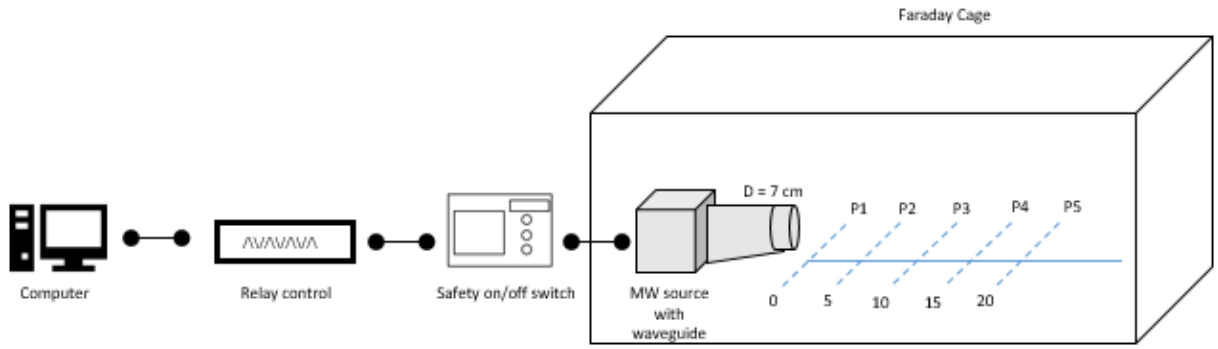

Figure 3: Vial setup with positions P1, P2, P3, P4 and P5 in front of the MW, indicated in cm (0-20 cm)

Table 2: Properties of the used vials

*Source: raepak.com	**Vial 1**		**Vial 2**
	PET		HDPE
dim. (lxwxd)	8x6x2.6	*[cm]*	8x6x3.7
Vol.	125 (+/- 2)	*[mL]*	175 (+/- 2)
*Rigidity - [0-5]	4		3
*Transparency - [0-5]	5		2
*Temp. resistance interval - cold	-40	*°C*	-79

*Temp. resistance interval - warm	55	*°C*	75

Table 3: Experiments conducted on the vials

	Position in front of MW [cm]	**Stirring**
Exp. 1	0, 5, 10, 15, 20	no
Exp. 2	0, 10, 20	yes

3.3 Core flood and EM heating setup and procedure

3.3.1 Core preparation

A 40.0 cm Bentheimer sandstone core which is cored from a large block is placed into an oven. After drying in the oven at 60 °C for 12 hours the core is prepared to be glued in. A priming grey glue layer made out of a mixture of an epoxy resin (Huntsman CW47) and a hardener (Huntsman REN HY33) is applied and left to dry for two days. Before gluing-in with the same mixture, it is vacuumed to remove air bubbles. The core is then placed into a mold and glued-in. Following this the mold is placed into an oven at approximately 60 °C for 2 hours and left to cool for at least 12 hours. The mold can then be removed and the core taken out. The dried glue layer is temperature resistant up to 180 °C, has a thickness of approximately 0.5 cm and functions as a lateral seal therefore leaving only the beginning- and endpoint of the core open to fluid flow. The glue penetrates into the core for approximately 1mm, reducing the clean rock diameter by 2 mm. This is accounted for at area and volume calculations. A 17 cm section is then cut to fit into the core holder. After being placed into the core holder and attached to the wave guide, the thermocouple entry points are drilled into the core and the four thermocouples are glued-in. The water tubes connected to the Quizix pump and backpressure unit are then connected to the core holder after which the setup is ready for initial water injection. After initial water injection each tube, nozzle, entry- and exit-point is checked for leakage. The sandstone core is then fully saturated with degassed tap water at room temperature, by injecting 10 PV.

3.3.2 EM core setup

Fig. 5 displays the schematic view of the experimental setup. A MW source is connected to a wave guide which guides EM radiation into the direction of the core holder and additionally limits the leakage of radiation to the surroundings. The MW, at the specific frequency, radiates with a wave length of 0.1224 m (Table 4). The connection between the wave guide and the MW has a conical shape with a diameter of 8 cm decreasing to 7 cm along its length of 9 cm. The

part of the wave guide containing the core holder is a cylindrical tube with a 7 x 19 cm (d x L) dimension (Fig. 6, left). The core, with a dimension of 4.0x17 cm (d x L) is placed into a PEEK core-holder with four holes drilled along its length for the fitting of four thermocouples (Fig. 6, left). The four thermocouples are placed at 2 cm, 5 cm, 9 cm, and 14 cm into the core. The thermocouples go through the wall of the core holder, penetrate approximately 1 cm into the core and are glued in place. Each thermocouple is made of a Nickel-Chromium/Nickel-Aluminum alloy with an accuracy of ± 0.2 °C and a response time of approximately 2.3 seconds. For each of the four thermocouples inside the core the assumption is made that the temperature readings are assigned to a 1 cm section of the core right before the thermocouple positions, as illustrated in Fig. 4.

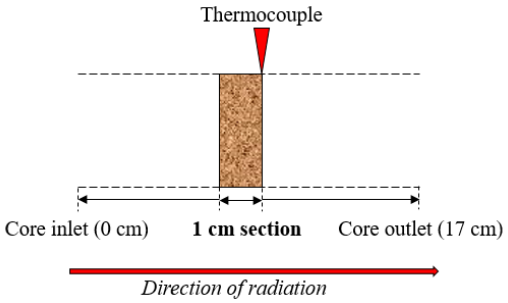

Figure 4: 1 cm section of the water saturated core at a thermocouple placed into the core. $m_{section} = m_w + m_{sst}$

A Quizix QS Series Precision Pump is used for water injection, to regulate the constant steady-state flow and the pressure inside the core. A backpressure is installed as a precautionary measure to check for leakage related pressure drop. Furthermore, a Temp-Press temperature acquisition system is installed which reads the temperature measured by the thermocouples and sends the data to the data acquisition unit and PC. The PC, which is used to start and stop the MW, can also be used for relay control. For each experiment the relay was kept constant. This particular setting results in an EM heating cycle as illustrated in Fig. 2. The water coming out of the core is collected without serving any other purpose. Finally, for safety related EM radiation hazard prevention, the core was placed in an aluminum box functioning as a Faraday cage (Fig. 6, right). The cage is insulated at the lid as well as all entry points of tubes and wires. This intends to contain all radiation within the cage to account for the main health, safety and environmental measures. Using a microwave leakage detector, the amount of radiation leakage along the Faraday cage and the core holder was measured. These values varied between 0.025 and 0.030 W/m^2, which is significantly below the human safety threshold of 1 W/m^2. Serving as an additional safety measure, an emergency stop switch is built into the lid of the Faraday cage. When the lid is opened, the switch detaches and automatically shuts off the power and thus

effectively shuts down the microwave. Table 4 provides the parameters related to the MW. Further details of the set-up used to conduct the experiments are reported by Paz et al., 2017, Kermen, 2011, and Hollmann, 2013.

Table 4: MW parameters

Symbol	Parameter/variable	Value	Unit (SI)
W	Microwave power	1000	[Watt]
f	Microwave frequency	2.45	[GHz]
λ	Wave length	0.1224	[m]

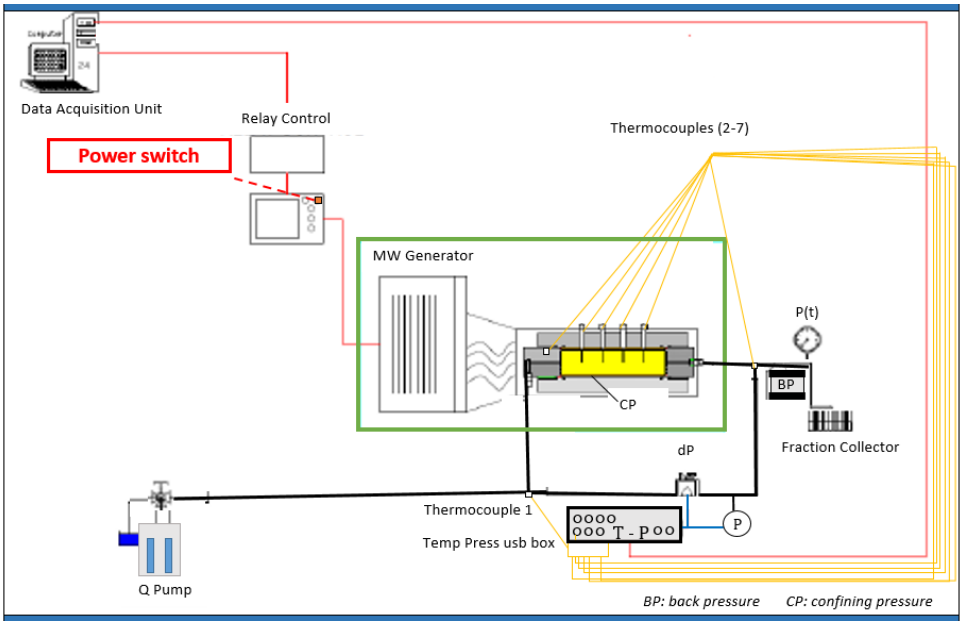

Figure 5: Schematic display of the experimental setup

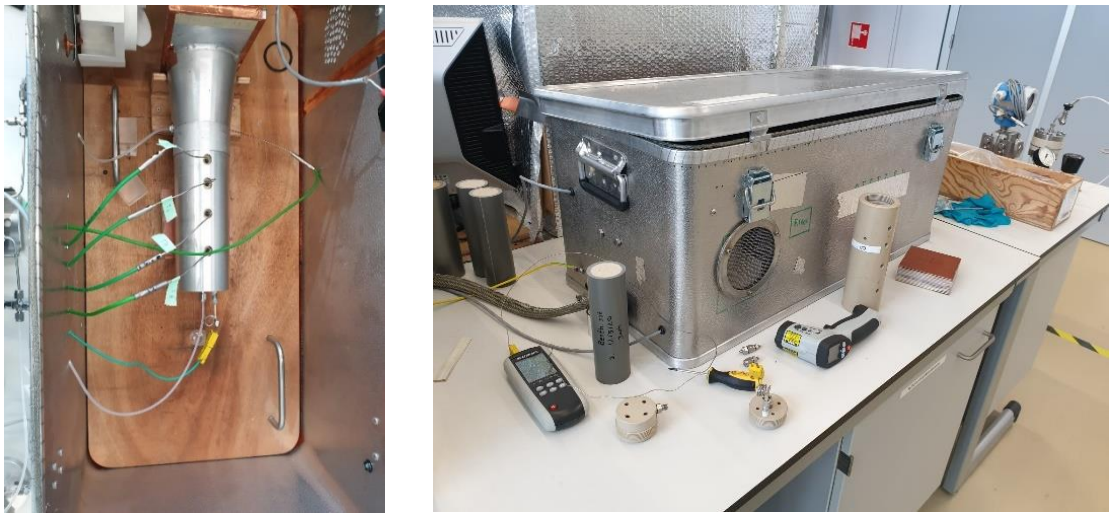

Figure 6: Left - Wave guide with conical connection to MW (top) and cylindrical tube with four thermocouple placement holes and **Right** - Aluminum Faraday cage with insulated lid, exit and entry points.

3.3.3 EM core experiments

Three experiments have been conducted on a water saturated sandstone core. During the experiments, the MW was turned on for 150 seconds consisting of 8 EM radiation cycles. After heating, the core was left to cool off during a 60 minute time span. During this whole procedure the temperature within the core is measured. The first experiment (Exp. 3) involves a fully water saturated core, at room temperature, subjected to EM heating at no-flow conditions. For the second (Exp. 4) and third (Exp. 5) experiment flow is induced at flowrates of 1 mL/min and 2 mL/min respectively. The temperature data obtained is used to gain insight into the temperature and energy profiles inside the system (water and rock). The reasoning behind the introduction of flow is to assess the effect that a marginal change from a static fluid regime to a (low flow rate) dynamic fluid regime has on the energy absorption and storage amount and rate inside the core. Table 5 presents information regarding the EM radiation times and fluid flow regimes for these experiments.

Table 5: Three core experiments subjected to EM heating

Experiment name	EM	EM time	Effective on-time	Cooling period	Flow	Flowrate
Exp. 3	yes	150 +/-1 sec	64 +/-1 sec	60 min	no	-
Exp. 4	yes	150 +/-1 sec	64 +/-1 sec	60 min	yes	1 mL/min (±1.5 PV)
Exp. 5	yes	150 +/-1 sec	64 +/-1 sec	60 min	yes	2 mL/min (±3 PV)

4 RESULTS

In this section we are going to discuss the results of both the EM characterization experiments as well as the heating of the porous media. Temperature and energy absorption profiles obtained from experimental data are provided and analyzed.

4.1 EM field characterization

Fig. 7 and 8 illustrate the temperature increase against the time of EM heating for vial 1 and vial 2 respectively. It is evident, first of all, that for every position at both vials the temperature increases linearly with time, within the experimental error. Secondly, the temperature increase (ΔT) of the water decreases with increasing distance from the MW source. In Fig. 7 a maximum temperature increase of approx. 30.0 ± 0.3°C is obtained at position P1 (0 cm in front of the MW) for vial 1. Vial 2 also reveals the largest temperature increase (approx. 17.0 ± 0.3°C) at position P1, closest to the MW source. The closer the vials are placed to the source, the higher the temperature increase. For vial

1 the effect of stirring does not significantly change the temperature profile at positions P3 and P5. At P1 however, the profile change for the stirring case is more evident at t = 120s and 150s. This looks like an anomaly and is assigned to being a result of inconsistent positioning of the thermocouple (by hand) in the vial when measuring the temperature. Following this, a more consistent placement of the thermocouple was implemented for all following measurements. Fig. 8 furthermore illustrates that stirring does not cause a large effect on the temperature profile of the water in vial 2.

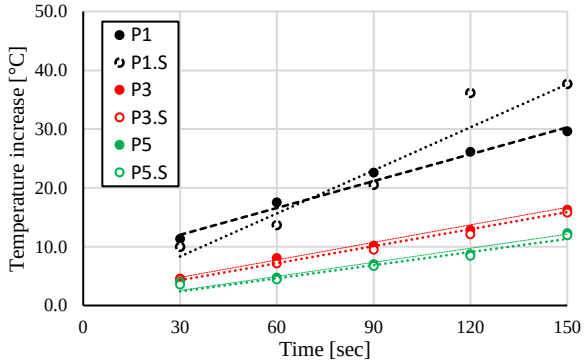

Figure 7: ΔT for vial 1 for 150 sec. of EM radiation. A comparison between the stirred and non-stirred case at 0cm, 10cm and 20cm from the MW source (Fig. 3). *ΔT Error: ± 0.3 °C.*

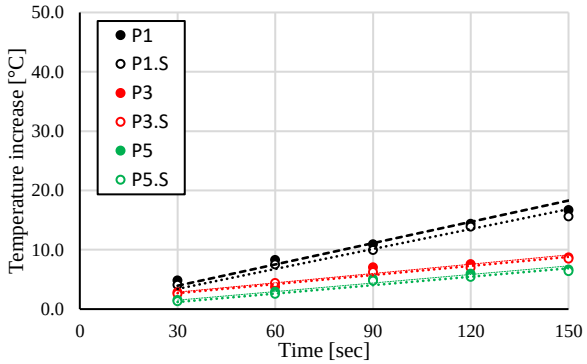

Figure 8: ΔT for vial 2 for 150 sec. of EM radiation. A comparison between the stirred and non-stirred case at 0cm, 10cm and 20cm from the MW source (Fig. 3). *ΔT Error: ± 0.3 °C.*

Fig. 9 and 10 illustrate the energy absorption by the water in the vials as a function of the distance from the MW source. It is evident that the energy absorption is largest closest to the MW source and declines exponentially with increasing distance from the MW source. Furthermore, it can be seen that for both the static and the stirred case the largest amount of energy is absorbed by vial 1, which has the smaller volume. This is in line with the expectation. The green values illustrate the percentage of energy absorbed by water after EM heating. For vial 1, the energy absorbed increases with 7% from the static case to when stirring is applied. However, this is not observed to be the case for vial 2. This contradiction could be assigned to the method used for measuring the temperature, as mentioned earlier. It is therefore not concise to draw a conclusion regarding the effect that stirring may have on energy absorption by water in the vials.

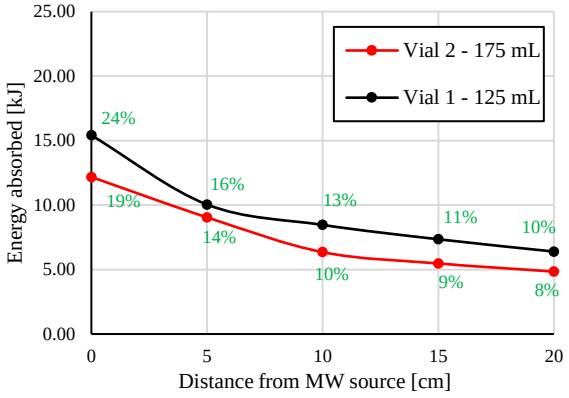

Figure 9: [No stirring]-Energy absorbed by water in vial 1 and vial 2 for 150 sec. of EM radiation. A comparison between both vials at 0cm, 5cm, 10cm, 15cm and 20cm from the MW source (Fig. 3). Energy absorption percentages by water indicated in green. [*E.abs error, vial1, vial2 (0 cm): ± 0.11 kJ, ±0.14 kJ || E.abs error, vial1, vial2 (20 cm): ± 0.59 kJ, ±0.77 kJ.*]

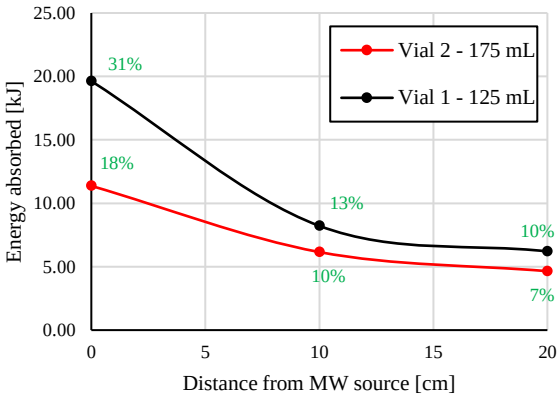

Figure 10: [Stirring]-Energy absorbed by water in vial 1 and vial 2 for 150 sec. of EM radiation. A comparison between both vials at 0cm, 10cm and 20cm from the MW source (Fig 3). Energy absorption percentages by water indicated in green. [*E.abs error, vial1, vial2 (0 cm): ± 0.03 kJ, ±0.04 kJ || E.abs error, vial1, vial2 (20 cm): ± 0.05 kJ, ±0.04 kJ.*]

4.2 EM heating experiments on core

4.2.1 No flow conditions

Fig. 11 reveals the development of the temperature inside the core during EM heating for the four thermocouples. The cyclicity of the heating process is evident which by the way corresponds to the heating cycles of the MW, illustrated by the black line. Furthermore, Fig. 11 reveals a linear increase in temperature corresponding to the linear temperature increase observed at the vial experiments. The thermocouple closest to the MW source (TC3) measures the highest temperature in the core after EM heating. Before EM radiation, the water in the core was at room temperature T_0 = 20.0 ± 0.2 C°. From Fig. 11 we can see that the temperature increases to approx. 72.0 °C , 64.0 °C , 44.0 °C and 33.0 °C for TC3, TC4, TC5 and TC6 respectively.

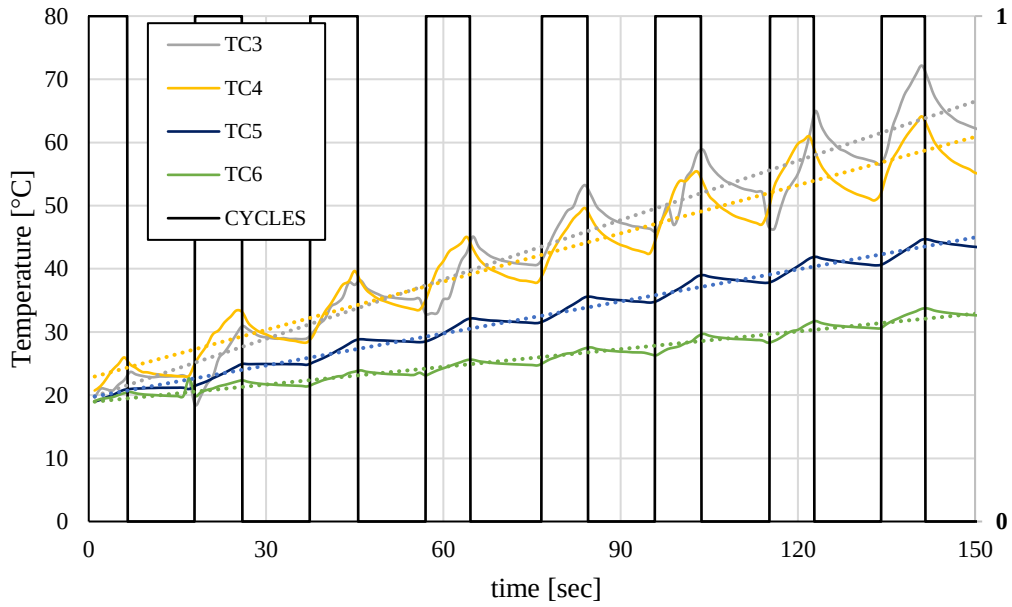

Figure 11: Core temperature as a function of time after approx. 150 seconds of MW activity. The eight MW cycles are visible for each of the TC positions. *No flow. Error in temp. measurement: 0.2 °C.*

Fig. 12 displays the temperature increase (*Δ*T), calculated for each EM cycle and plotted as a function of each TC position. It can be observed that the largest increase in temperature is obtained close near the inlet of the core. Furthermore, the *Δ*T values exponentially decline along the length of the core, again corresponding to the results obtained at the vial experiments.

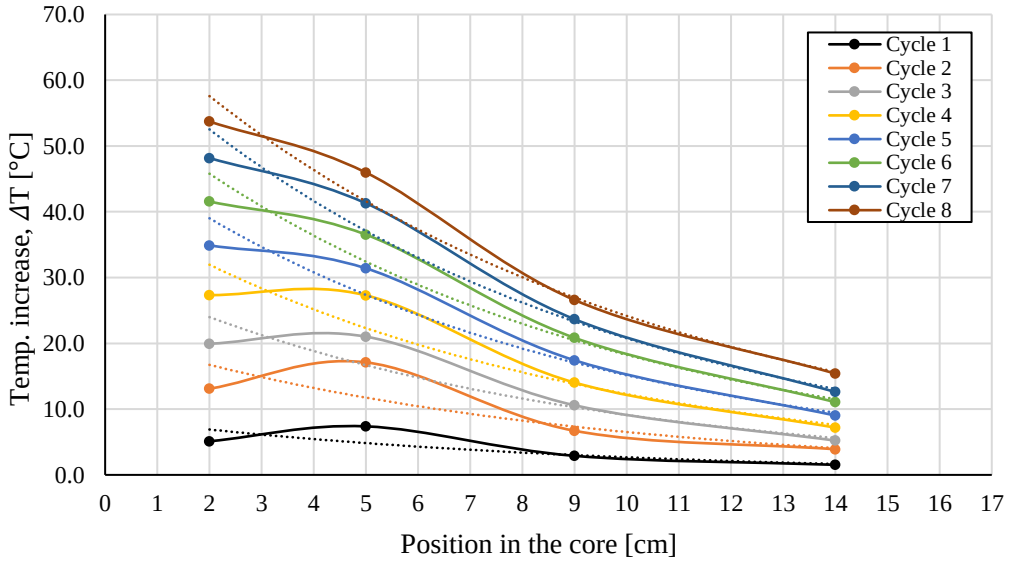

Figure 12: *Δ*T profile for eight MW cycles, based on four temperature data points, along the length of the core. The resulting trend lines are also displayed. *(TC3, TC4, TC5 and TC6 at 2, 5, 9 and 14cm in the core). Error in. ΔT values: 0.3 °C.*

The resulting trend lines at Fig. 12 are used to obtain the ΔT values for the remaining positions along the core. These ΔT values are then used to calculate the energy absorbed by the water and rock during EM heating. Fig. 13 illustrates 1 - the cumulative amount of energy absorbed by the core as a whole as a function of increasing MW cycles (green line and axes) and 2 - the gradually increasing amount of energy along the length of the core for eight EM cycles. The highest amount of energy is absorbed at the inlet of the core (approx. 2.41 ± 0.02 kJ) declining in the direction of the core outlet. This is consistent with what we have seen at the experiments with the vials, where we observed that the EM field is decaying near exponentially with increasing distance from the source (Fig. 9 and 10). The green line illustrates the linearly increasing amount of energy absorbed by the core as a whole, which is corresponding well to the linearly increasing temperature profiles seen in Fig. 11. At the end of EM heating, approx. 19.79 ± 0.02 kJ is absorbed by the water and the rock together. Compared to the energy generated this results in an energy absorption percentage of 31%.

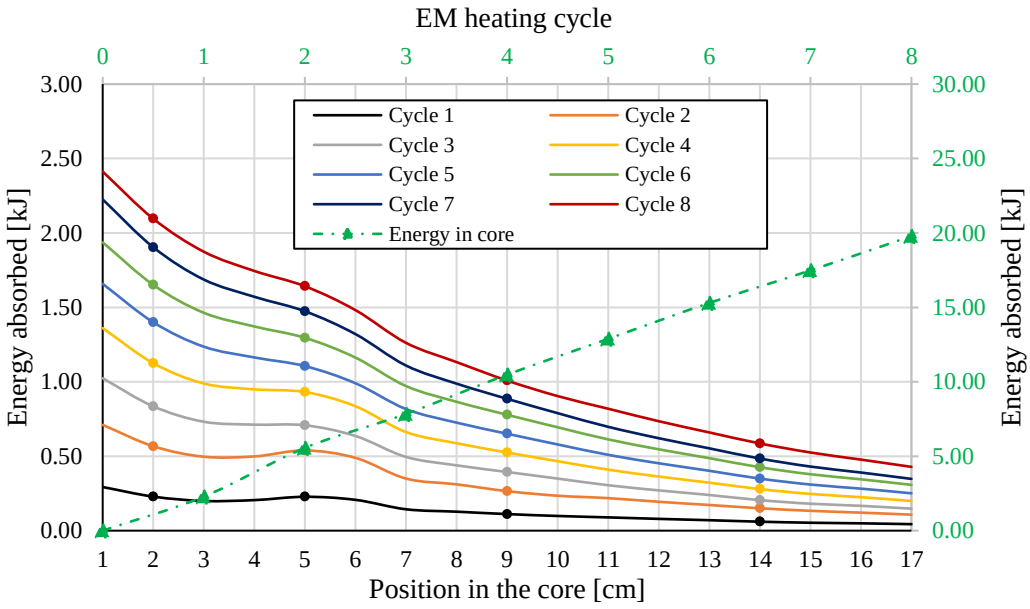

Figure 13: Energy absorption profile along the length of the core. The green line displays the cumulative amount of energy in the whole core, linearly increasing with each EM cycle. Approx. 19.79 ± 0.02 kJ after eight cycles. *(TC3, TC4, TC5 and TC6 at 2, 5, 9 and 14cm in the core)*

4.2.2 EM heating under flow conditions: 1 mL/min

Fig. 14 illustrates the temperature profile for Exp. 4, where flow is introduced at a rate of Q = 1 ml/min. Water flooding is implemented during EM heating as well as the 60 minute cooling-off period. Similarly to Exp. 3 the temperature increases linearly versus time. It can be seen that for TC4, situated at 5 cm into the core, the maximum temperature increases slightly after EM heating compared to Fig. 11. For TC5 and TC6, several spikes in temperature are visible.

This is assumed to be the result of interference of the EM-field on the conducting part of the thermocouples. By using optical thermocouples this effect may be removed. However, the analysis of this occurrence is not a part of this study.

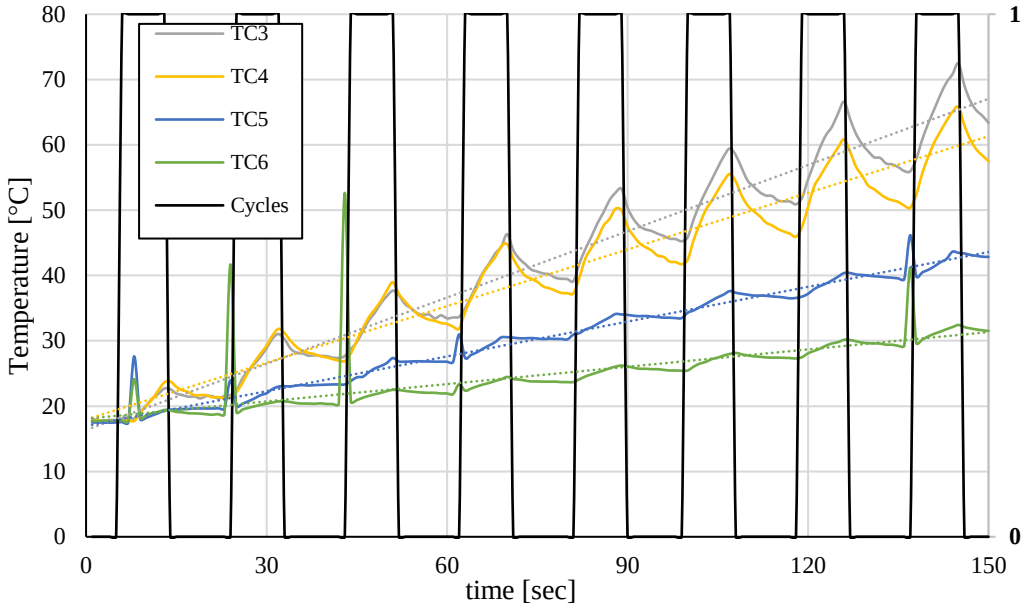

Figure 14: Core temperature as a function of time after approx. 150 seconds of MW activity. The eight MW cycles are visible for each of the TC positions. *Q = 1 mL/min. Error in temp. measurement: 0.2 °C.*

Fig. 15 displays the temperature increase (ΔT), similar to Fig. 12. It can be observed that the rate of decline of ΔT after eight EM heating cycles, between TC3 and TC 4, is marginally smaller compared to the case of no flow. The slope is less steep. The rate of decline of ΔT in between TC4 and TC5 however, is slightly steeper compared to the case of no flow. This effect is deemed to be the result of the introduction of flow.

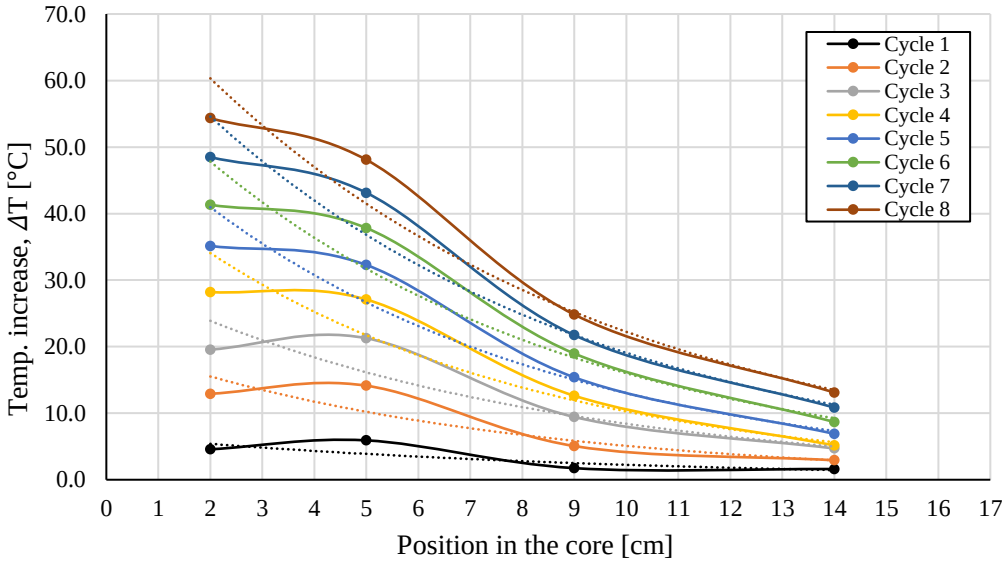

Figure 15: ΔT profile for eight MW cycles, based on four temperature data points, along the length of the core. The resulting trend lines are also displayed. *(TC3, TC4, TC5 and TC6 at 2, 5, 9 and 14cm in the core). Error in. ΔT values: 0.3 °C.*

Using the data illustrated in Fig. 15, the corresponding energy absorbed by the water and rock along the length of the core as well as cumulatively during the eight EM heating cycles is calculated and provided in Fig. 16. The highest amount of energy is again absorbed at the inlet of the core (approx. 2.59 ± 0.02 kJ) declining in the direction of the core outlet. Energy absorption of approx. 19.41 ± 0.02 kJ is measured which results in an energy absorption percentage of 30%. Compared to the previous experiment of no flow, the difference is marginal.

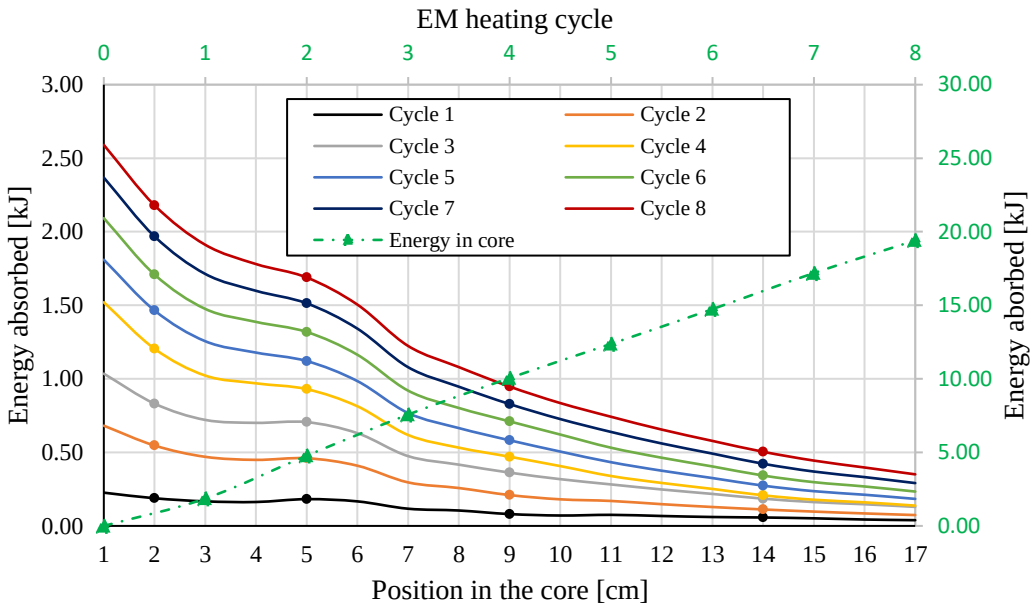

Figure 16: Energy absorption profile along the length of the core. The green line displays the cumulative amount of energy in the whole core, linearly increasing with each EM cycle. Approx. 19.41 ± 0.02 kJ after eight cycles. *(TC3, TC4, TC5 and TC6 at 2, 5, 9 and 14cm in the core)*

4.2.3 EM heating with increased flow conditions: 2 mL/min

Fig. 17 illustrates the temperature profile for Exp. 5, where flow is increased to Q = 2 ml/min. Similarly to Exp. 3 and 4, the temperature increases linearly versus time. Even at this flow rate the temperature in the core reaches values comparable to the previous two core experiments. The flow of water at this flow rate does not seem to affect the heating of the water. This is what is desired when combining EM heating with core flooding. The heating of the water should not be compromised by too high of a flow rate. This may result is a delay of heating, causing heating of the water to occur further from the core inlet. Also visible in Fig. 17 are severe spikes for TC5 and TC6, most likely due to hot spot generation at TC-core contact points.

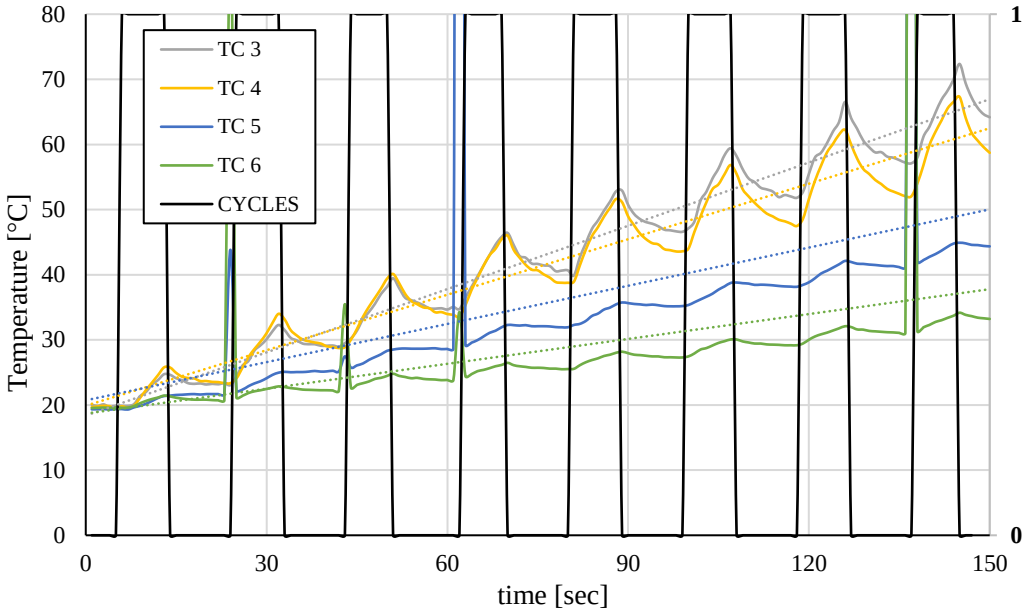

Figure 17: Core temperature as a function of time after approx. 150 seconds of MW activity. The eight MW cycles are visible for each of the TC positions. *Q = 2 mL/min. Error in temp. measurement: 0.2 ℃.*

Fig. 18 displays the temperature increase (*Δ*T), similar to Fig. 15 and Fig. 12. It can be observed that the rate of decline of *Δ*T after eight EM heating cycles, between TC4 and TC 5, is marginally larger compared to the case of flow at 1 mL/min and no flow. The slope is steeper. This effect is deemed to be the result of the introduction of flow.

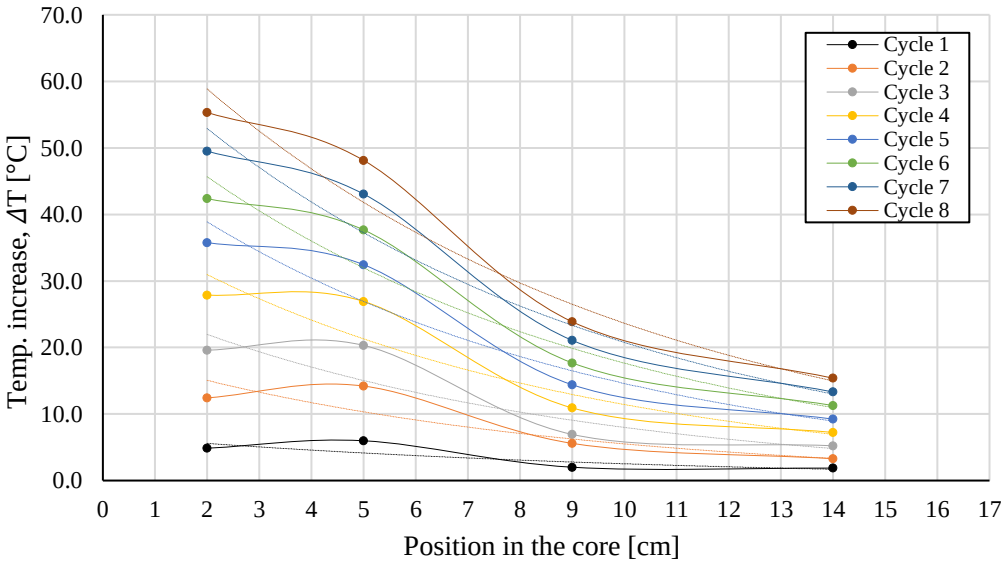

Figure 18: Temperature profile for eight MW cycles, based on four temperature data points at 2cm, 5cm, 9cm and 14cm in the core. The resulting trend lines are also displayed. *(TC3, TC4, TC5 and TC6 at 2, 5, 9 and 14cm in the core). Error in. ΔT values: 0.3 ℃.*

The energy absorption, per cycle as well as cumulatively in the core as a whole, is calculated and provided in Fig. 19. The largest amount of energy is absorbed at the inlet of the core (approx. 2.49 ± 0.02 kJ). For the core as a whole, an approximate amount of 19.77 ± 0.02 kJ is absorbed. Compared to the energy generated this results in an energy absorption percentage of 31%.

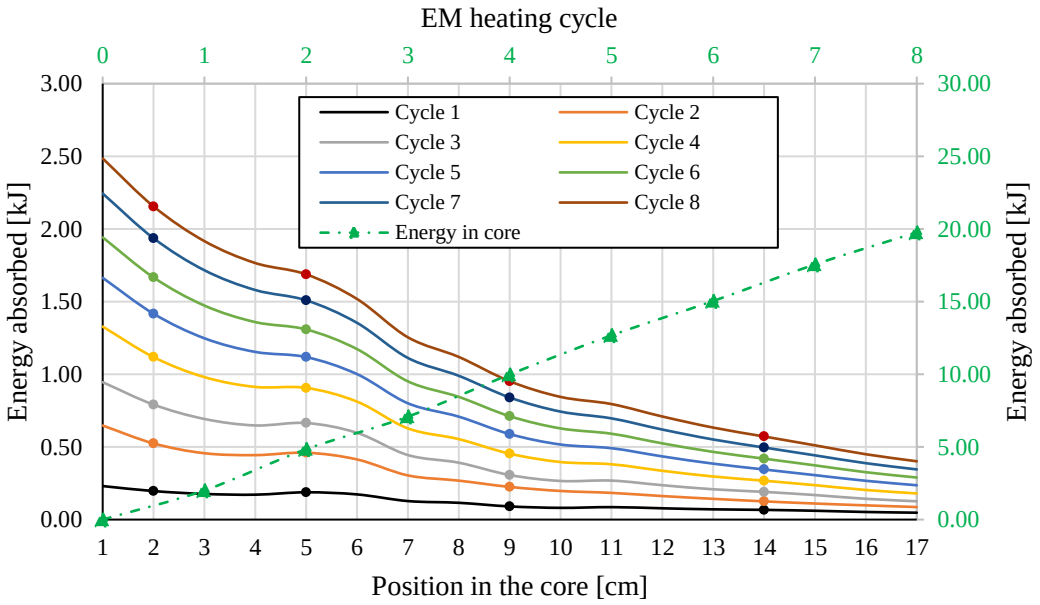

Figure 19: Energy absorption profile along the length of the core. The green line displays the cumulative amount of energy in the whole core, linearly increasing with each EM cycle. Approx. 19.77 ± 0.02 kJ after eight cycles. *(TC3, TC4, TC5 and TC6 at 2, 5, 9 and 14cm in the core)*

.

4.3 Cooling-off period after EM heating

After turning off the MW, the setup is left to rest for one hour. The thermal energy losses and subsequent storage is studied as a function of time (one hour), with 10 minute increments, as well as for the distance along the core.

4.3.1 Cooling-off - No flow

Fig. 20 illustrates the temperature versus the time during the cooling period under no flow conditions. It can be observed that the temperature declines exponentially until a stable temperature of around 32.0 ± 0.2 °C is reached. Based on this data the energy decline within the system (core and water together) is evaluated.

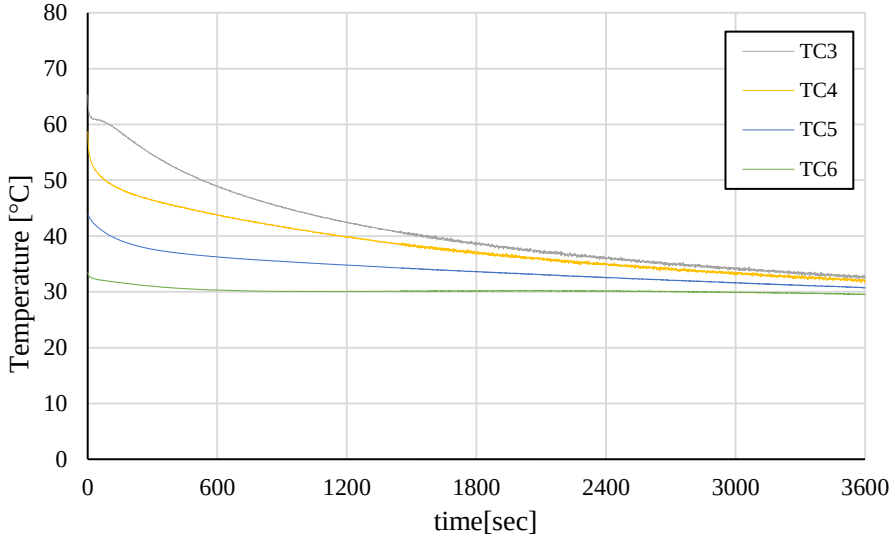

Figure 20: Temperature decline profiles for TC3, TC4, TC5 and TC6 immediately after EM heating, for the duration of 60 minutes. *For the no flow case. Error in temp. measurement: 0.2 °C.*

Fig. 21 illustrates the energy storage profile for Exp. 3. Under the no-flow condition, energy decline along the length of the core is displayed for 60 minutes, with ten minute increments. The largest thermal energy losses occur near the core inlet (TC3, at 2 cm). After 60 minutes the energy along the length of the core is largely constant at approx. 0.50 ± 0.02 kJ. Additionally, the red curve illustrates the exponentially declining cumulative energy profile within the core as a whole. Based on this, it can be observed that 60% of the energy in the core is dissipated after 60 minutes. This results in energy storage, at this point in time, of 40% which translates to 7.83 ± 0.02 kJ.

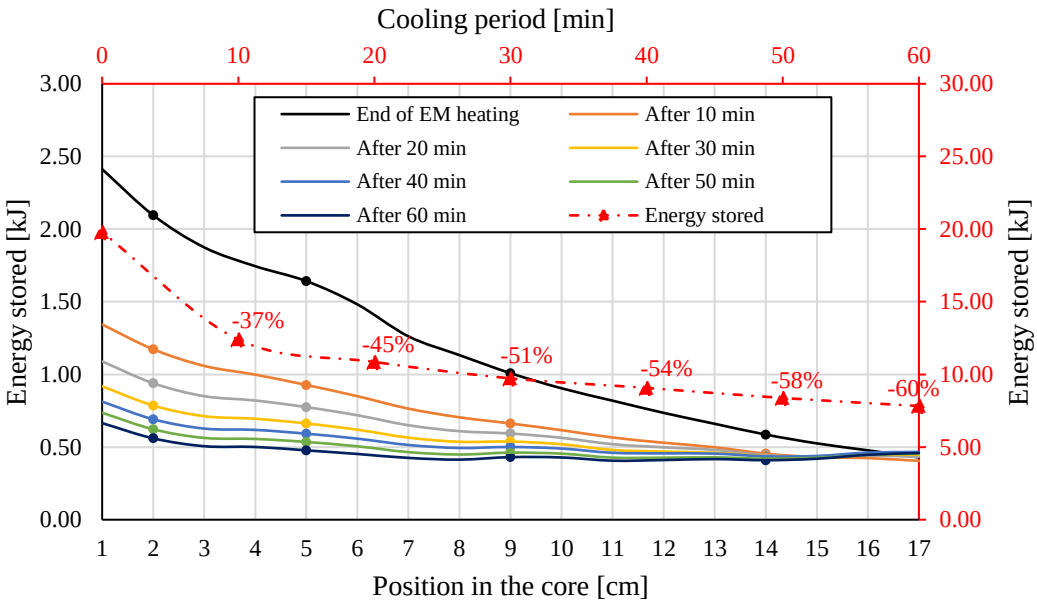

Figure 21: Energy storage profile along the length of the core. Red line displays the cumulative amount of energy in the whole core. Thermal energy losses of approx. 60% after 60 minutes. *(TC3, TC4, TC5 and TC6 at 2, 5, 9 and 14cm in the core). Error in energy stored values: 0.02 kJ.*

4.3.2 Cooling-off - Flow at 1 mL/min

Fig. 22 illustrates the temperature decline profile for Exp. 4. Compared to Fig. 20 corresponding to Exp. 3, a higher rate of temperature decline for TC3 and TC4 can be observed. TC5 and TC6, placed further along the core, largely demonstrates the same rate of decline. This is deemed to be the effect of water injection on the rate of energy decline within the system. By increasing the flowrate further, this effect should be enhanced. A constant temperature within the system is reached around the 45 minute (2700 sec.) mark, at approx. 30.0 °C.

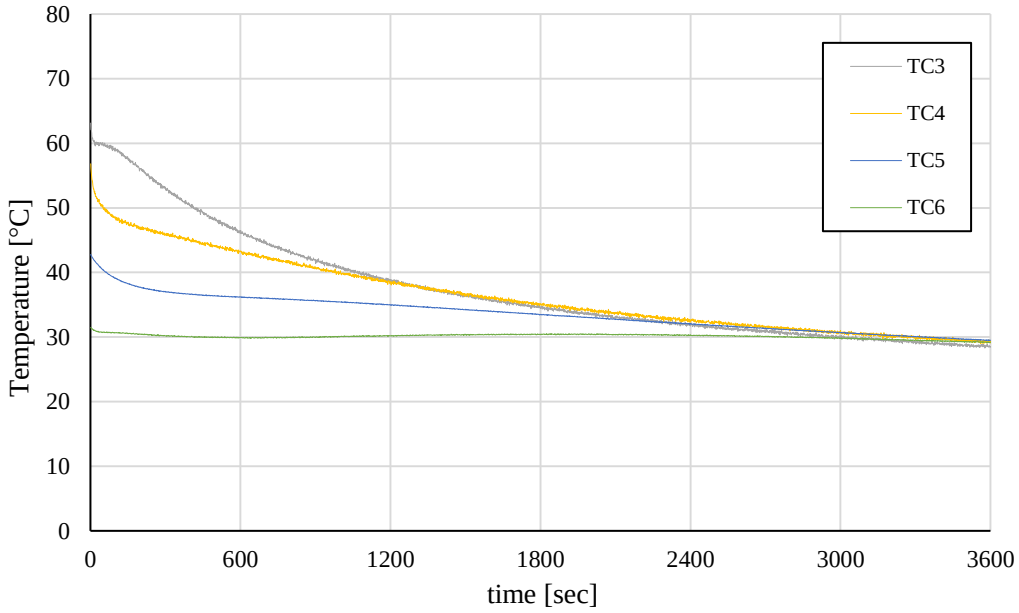

Figure 22: Temperature decline profiles for TC3, TC4, TC5 and TC6 immediately after EM heating, for the duration of 60 minutes. *Flow at 1 mL/min. Error in temp. measurement: 0.2 °C.*

Fig. 23 illustrates the energy storage profile for experiment Exp. 4. Similar to Exp. 3, the largest thermal energy losses occur near the core inlet (TC3). After 60 minutes the energy along the length of the core is largely constant at approx. 0.40 ± 0.02 kJ. The red exponentially declining cumulative energy profile illustrates that 68% of the energy in the core is dissipated after 60 minutes. This is higher compared to Exp. 3, which again indicates the effect that flow has on energy decline within the core. In this case, energy storage of approx. 32% is achieved which translates to approx. 6.17 ± 0.02 kJ.

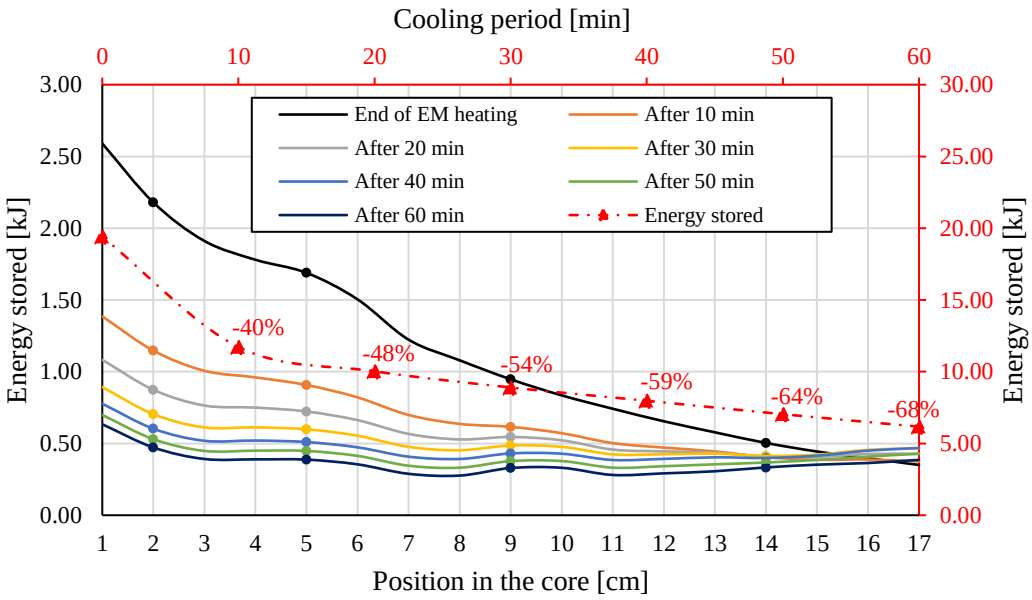

Figure 23: Energy storage profile along the length of the core. Red line displays the cumulative amount of energy in the whole core. Thermal energy losses of approx. 68% after 60 minutes. *(TC3, TC4, TC5 and TC6 at 2, 5, 9 and 14cm in the core). Error in energy stored values: 0.02 kJ.*

4.3.3 Cooling-off - Flow at 2 mL/min

The temperature decline profile for Exp. 5 is illustrated by Fig. 24. A higher rate of temperature decline is observed compared to Exp. 3 and Exp. 4. After 30 minutes (1800 sec.) the system has reached a constant temperature of approx. 32.0 C°. From this point in time, the temperature within the length of the core declines further as a whole. This is an enhanced effect related to the increase in flowrate.

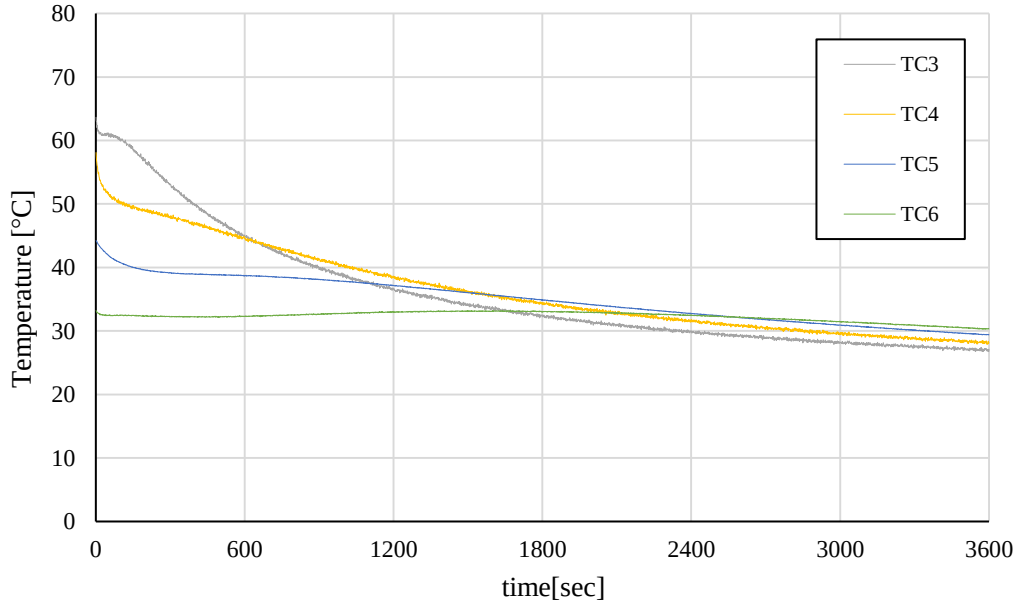

Figure 24: Temperature decline profiles for TC3, TC4, TC5 and TC6 immediately after EM heating, for the duration of 60 minutes. *Flow at 2 mL/min. Error in temp. measurement: 0.2 °C.*

As Fig. 25 illustrates, energy to the amount of approx. 0.30 ± 0.02 kJ is stored along the length of the core after 60 minutes. Cumulatively, for the system as a whole, the red profile for thermal energy losses reveals an energy decline of approx. 77%, which translates to an energy storage amount of approx. 4.55 ± 0.02 kJ or 23%.

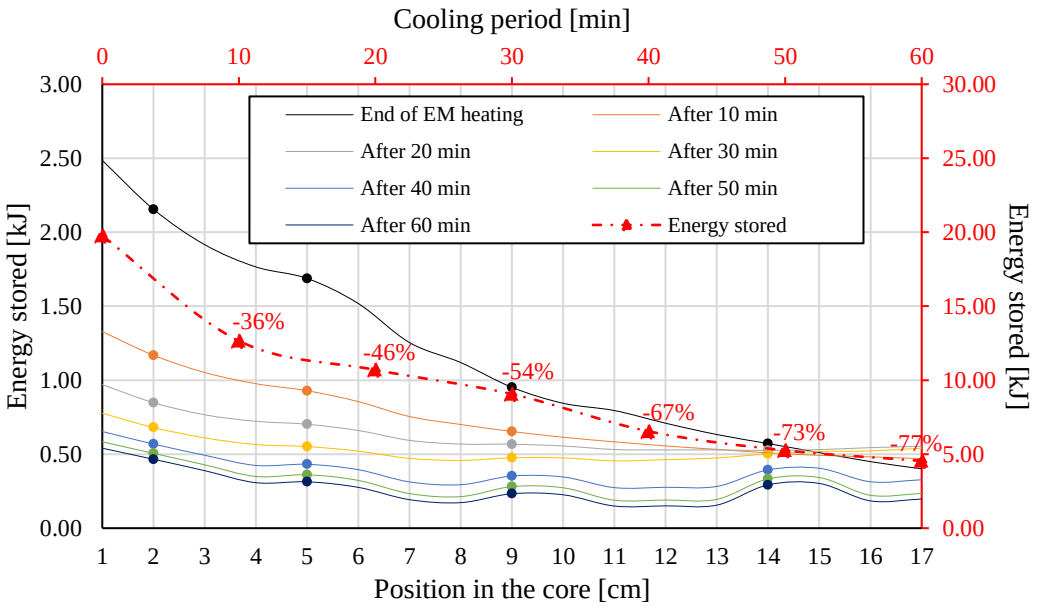

Figure 25: Energy storage profile along the length of the core. Red line displays the cumulative amount of energy in the whole core. Thermal energy losses of approx. 77% after 60 minutes. *(TC3, TC4, TC5 and TC6 at 2, 5, 9 and 14cm in the core). Error in energy stored values: 0.02 kJ.*

5 CONCLUSIONS AND RECOMMENDATIONS

5.1 Conclusions

At the beginning of this study the objective was to gain insight into the energy absorption and storage after EM heating on a porous medium. The experiments that were conducted have provided results from which the following conclusions are drawn:

- When water in the vials is heated by EM radiation, a significant and measurable linear increases in temperature versus time is achieved. Based on these results we can subsequently determine the profile of energy absorption.
- Substantial amounts of energy absorption in the core have been obtained which assumes promising signs for EM heating of a water saturated core. The introduction of flow during EM heating did not diminish the energy absorption by water inside the core.

- After a one hour cooling period a large amount of the absorbed energy in the core is lost in the form of thermal energy losses. However, a significant amount of energy remains stored in the core. The energy storage value obtained is the highest for the no flow case and decreases with increasing flowrate.
- The effect of flow on energy storage inside the core illustrates that the chosen flowrate should be subject to caution in order to prevent the EM heating method to decline in efficiency and thus diminishing its purpose.
- Our results suggest that EM heating, with further improvements and more in depth analysis, is potentially a viable technology for thermal energy storage purposes.

5.2 Recommendations

To enhance the quality of the data and enable their more detailed interpretation the following improvements are recommended:

- To optimize the effectiveness of energy generation, and subsequently the energy absorption and storage, a higher quality MW source should be used instead of the conventional microwave source.
- In order to reduce the large amounts of thermal energy losses, the insulation of the experimental setup should be improved.
- In order to eliminate EM interference on the thermocouples the use of optical thermocouples is recommended.

REFERENCES

Abernethy, E.R. Production increase of heavy oils by electromagnetic heating. *Journal of Canadian Petroleum Technology*, pages 91-97 (1976)

Almeida, S.O.d., Zitha, P.L.J. & Chapiro, G. A Method for Analyzing Electromagnetic Heating Assisted Water Flooding Process for Heavy Oil Recovery. *Transp Porous Med* (2021)

Hollmann, T. EM Stimulated Water Flooding In Heavy Oil Recovery. *MSc. Dissertation TU Delft*, pages 1-76 (2013)

Kermen. E. Thermal enhancement of water flooding in medium-heavy oil recovery. *MSc Dissertation TU Delft*, pages 1-45 (2011)

Molecular Cell Biology, *Sixth Edition, W. H. and Company* (2008)

Paz, P., Hollmann, T., Kermen, E., Chapiro, G., Slob, E., & Zitha, P. EM Heating-Stimulated Water Flooding for Medium-Heavy Oil Recovery. *Transport in Porous Media*, 119 (1), pages 57-75 (2017)

Peksa, Anna E., Wolf, Karl-Heinz A.A., Zitha, Pacelli L.J. Bentheimer sandstone revisited for experimental purposes. *Marine and Petroleum Geology*, 67, pages 701-719 (2015)

Samanta. Theoretical analysis on microwave heating of oil-water emulsions supported on ceramic, metallic or composite plates. *International Journal of Heat and Mass Transfer*, pages 6136-6156 (2007)

Tran, T.S., Zitha, P.L.J., De Rouffignac, E. Electromagnetic Assisted Carbonated Water Flooding for Heavy Oil Recovery. *World Heavy Oil Congress 2009 Proceedings* (2009)